Modeling Atmospheric Activity of Cool Stars

Carolus J. Schrijver

Lockheed Martin Advanced Technology Center
L9-41/252, 3251 Hanover Street, Palo Alto CA 94304, USA

Abstract. This review discusses a set of simple models for cool-star activity with which we compute (1) photospheric field patterns on stars of different activity levels, (2) the associated outer-atmospheric field configurations, and (3) the soft X-ray emission that is expected to result from the ensemble of loop atmospheres in the coronae of these stars. The model is based on empirically-determined properties of solar activity. It allows us to extrapolate to stars of significantly higher and lower activity than seen on the present-day Sun through its cycle. With it, we can, for example, gain insight into stellar field patterns (including a possible formation mechanism for polar starspots), as well as in the properties of coronal heating (helpful in the identification of the quiescent coronal heating mechanism). Lacking comprehensive theoretical understanding, the model's reliance on empirical solar data means that the multitude of processes involved are approximated to be independent of rotation rate, activity level, and fundamental stellar parameters, or – where unavoidably necessary – assumed to simply scale with activity. An evaluation of the most important processes involved guides a discussion of the limits of the model, of the limitations in our knowledge, and of future needs.

> "I propose to adopt such rules as will ensure the testability of scientific statements; which is to say, their falsifiability."
>
> *Karl Popper (1902-1994)*

1. Introduction

By any measure, our knowledge about magnetic activity of stars in general, and of the Sun in particular, continues to increase rapidly. A fleet of spacecraft and a variety of ground-based observatories enable us to scrutinize stars with ever increasing sensitivity, spectral resolution, and angular resolution. Tenacity towards time-allocation panels has also paid off: data bases on some stars stretch back for almost two decades in the ultraviolet and in X-rays, and even more in the optical. Unfortunately, the temporal coverage is generally limited to a series of irregularly timed, short observing runs, spectra generally cover only a restricted pass band at a time, and angular resolution useful for the study of cool stars like the Sun is only approximated by (Zeeman) Doppler imaging or eclipse mapping which leave considerable ambiguity in the reconstructed images.

As in any field of science, we see that new observational evidence, advancing analytical work, and state-of-the-art numerical studies make our earliest ideas obsolete, and even as we struggle to patch the fabric of our thinking, holes are torn in it as new questions arise. We would like to think in terms of the classical philosophy of physics, i.e., to think in terms of linear superpositions of simple phenomena that can be studied in isolation, á la Descartes. Solar and stellar studies are presenting the unavoidable reality, however, that the stars that we are attempting to understand are non-linear, non-local, non-stationary systems, with disjoint interfaces – often with feedback loops – between the various domains, in an inherently 3D geometry.

Has our understanding kept up with our knowledge? The answer to that question depends on how we measure understanding. We may ask whether we can demonstrate that we can model our object of study in detail. We are clearly a long way off from that kind of understanding. More realistically, and also more pragmatically, we can ask the following question: do we have the quantitative means to test (i.e., to attempt to falsify in Popper's philosophy) some composite model that is based on sets of known phenomena, when it is applied to situations other than those used to establish the rules upon which it is based? If that model is a non-trivial endeavor to capture what we know, then establishing where the model fails will provide us with new understanding or at least points out where the limits or our understanding lie. Currently, we have prototype model components for the whole of stellar magnetic activity, albeit that they are mostly stand-alone units that can be only used to feed information from one process to the next. Ultimately, a full model would need to contain feedback loops to reflect the close coupling of many processes.

At the meeting, the charge for this review was to address "physical processes." To do justice to all topics that fall under that header even in the strictest interpretation is impossible in one review, or even in a full-sized book. Instead, I focus on a discussion of a bare-bones model of stellar magnetic activity as a guide to identify some of the many limitations in our knowledge and understanding of stellar magnetic activity. This model is based on the only example of stellar magnetic activity that we can observe in detail, namely the Sun, and is applied to, and tested against, stars outside the range of activity of the present-day Sun. It comprises only the photospheric field, a potential-field corona, and loop atmospheres, but even so uncovers interesting phenomena when applied to stars.

The model is described in detail in the studies by Schrijver (2001), Schrijver and Title (2001), and Schrijver and Aschwanden (2001), referred to as papers I, II, and III, respectively. These papers provide many references to related work upon which they build; this review only gives select references that are most relevant to the synthesis as presented here. The foundation of the surface-diffusion model was developed by Sheeley and colleagues (e.g., DeVore, 1987, Sheeley *et al.*, 1987), who demonstrated its viability, and who explained many solar features with it. In order to keep the reference list from becoming too long, long-known phenomena are often left without a reference.

How do we extrapolate solar activity sensibly to other stars? In this paper, I start from the premise that there are no differences from the baseline – solar – case, and scale properties with activity level only where undeniably needed. In

the process, it will become clear that we can discuss properties of the deep-seated dynamo as well as of the mechanism(s) for outer-atmospheric heating that would not otherwise have been accessible to scrutiny, primarily because the model allows us to look at stellar activity from a systems perspective.

2. A Model for Solar and Stellar Activity

In order to model the magnetic activity of any star, one has to have at least knowledge (1) of the source function for photospheric magnetic flux (i.e., on the products of the dynamo that penetrate the surface), (2) of the mechanism(s) that disperse field within the photosphere and that remove it from there, (3) of the formation and evolution of the field patterns on the stellar surface, (4) of the extension of the magnetic field into the outer atmosphere, and (5) of the transport of radiative and non-radiative energy into, within, and out of the outer atmosphere. Aspects of each of these topics are discussed in the following subsections.

2.1. The dynamo as the source of activity in stellar atmospheres

The dynamo process

The functioning of the dynamo remains one of the biggest mysteries in our field. There are rudimentary models that at least reproduce the solar butterfly diagram. However, our understanding of the dynamo process does not (yet) provide us with adequate understanding of how that pattern depends on stellar parameters, or indeed whether there is such a pattern under all circumstances. Nor can we derive what the mean level of activity is as a function of rotation and other parameters, or how stellar variability evolves on a time scale of years to decades.

The first step to take for the current purpose of modeling stellar atmospheric activity is to determine how the stellar parameters (including rotation) determine the mean activity level of the star. Here we run into problems immediately. We have empirical evidence (e.g., Noyes *et al.*, 1984) that the mean level of cool-star activity depends on the dimensionless Rossby number, which measures the relative effect of stellar rotation on convective motions. The Rossby number is, strictly speaking, a local quantity, being the ratio of the convective turnover time scale to the local rotation period. The latter is not likely to differ substantially throughout the convective envelope, as differential rotation appears to be limited to a moderate fraction of the rotation period. The convective turnover time, however, differs by ~ 3.5 orders of magnitude between top and bottom of the convective envelope for a Sun-like star. Most studies assume that the large-scale dynamo operates predominantly in the deeper layers of the convective envelope, and observational studies do indeed support the use of the turnover time characteristic for the bottom layers of the convective envelope, at least for main-sequence stars.

Numerical studies suggest, however, that dynamo action occurs everywhere within convective domains of ionized gas. In a strongly stratified medium, such as a stellar convective envelope, the convective length and time scales depend markedly on depth. As field is transported from one depth to another (in gradually overturning convection, subject to buoyancy and to the effects of the co-

herent, fast downdrafts), the layers and their scales are unavoidably coupled. Combine this with the fact that convective turnover time, effective temperature, envelope volume, and stellar mass are all monotonically related to each other along the main sequence, and the problem of disentangling the impact of each of these parameters becomes clear (compare Pizzolato *et al.* in these proceedings). Evolved stars and tidally-interacting binary stars do not conform to the simple Rossby-number scaling, and these therefore likely point out that other parameters are also involved in determining the level of a star's activity.

The high magnetic activity in fully convective T Tauri stars demonstrates that the convective overshoot layer, so prominent in most current models of the solar dynamo, is clearly not essential to the functioning of an efficient dynamo. Whereas one may speculate that some other form of a dynamo (perhaps turbulent instead of ordered) works in fully convective stars, stellar observations suggest that there is no significant transition in the properties of activity around the mass where main-sequence stars are expected to become fully convective (see Mullan, these proceedings, on the question of deep convection in these coolest stars). This means that either there is a smooth transition from one mode to the other with deepening convection, or the overshoot layer is not all that important because most of the action in fact occurs within the convective envelope itself, even for stars like the Sun. Work by Dorch and Nordlund (2001; see also Tobias *et al.* (2001)) supports the latter. They show that the asymmetry between the convective upflows and downdrafts pumps field towards the bottom of the convective envelope, on average just about balancing the buoyancy-driven upward flux of field. This results in a distribution with increasing flux with increasing depth, with only some of the flux being pumped into, and stored within, the overshoot layer. It is interesting that such a significantly different idea than the fashionable view that the dynamo is primarily active in the overshoot layer finds experimental support. Once solar and stellar researchers have advanced from their views in a joint effort to understand the dynamo, we may find that we have moved away significantly from the current concept of the overshoot dynamo.

Given that there is no adequate dynamo theory that relates activity to stellar parameters, we apply our model only to single, main-sequence stars, use the empirical rotation-activity relationship to calibrate activity to stellar rotation rate (necessarily in that direction), and restrict our application to stars of moderate to low activity to avoid the additional problem of dynamo saturation.

Time-dependence of activity

Once the mean activity level has been set, we have to decide how the rate of flux emergence for the model star is modulated with time on the time scale of years to decades. Although there is evidence that cycle periods are related to rotation periods and Rossby numbers (e.g., Saar and Brandenburg, 1999), there is much scatter and discussion about these trends. The utilization of theoretical constraints is hampered by the fact that current dynamo models are often linear or, if they are not, that their nonlinearity rests on rather ad-hoc choices about the parameterization of the coupling between plasma flows and magnetic field. Moreover, cyclic modulation of activity appears not to be the most common state to be in, even for a star like the Sun at a comparable activity level: only one in three Sun-like stars has a clear cycle modulation (Baliunas *et al.*, 1995). This fraction may be somewhat larger than what we find based on Ca II K

monitoring because some diagnostics apparently show cycles where others may not (Saar, private communication), but clearly this information indicates that a solar-like dynamo often is in another state than the simply cycling one. The absence of clear empirical or theoretical guidance prompted us to adopt a cycle period and time profile like those of the Sun in our modeling.

Flux spectrum

Next, we need to inject flux into the photosphere. Extensive studies of solar activity have allowed us to extract the patterns in the emergence of active regions, in position, time, and size, including the clustering of successive, cospatial regions. These statistics include the well-known Hale polarity rule (opposite leading polarities on opposite hemispheres, and in subsequent spot cycles within the same hemisphere), and Joy's rule (the leading polarity tends to emerge somewhat closer to the equator than the following polarity), including the increasing spread with decreasing region size (Harvey, 1993). Studies of earth-based diurnal observations and of space-based (nearly) continuous observations have allowed us to extend these distributions downward to the ephemeral regions (e.g., Harvey, 1993; Hagenaar, 2001). Only the properties of the smallest concentrations, known as the weak field or the innernetwork field, still elude us.

Information on the properties of emerging flux are known essentially only for the Sun. How to extrapolate that information to different stars, or even to stars of solar type but of different levels of activity? One plausible Ansatz is suggested by some of the most remarkable diagrams in our field: the power-law relationships between flux densities from, for example, the chromospheres and coronae of cool stars extend over a factor of approximately 100,000 in soft X-rays without significant dependence on stellar effective temperature or surface gravity, except for the coolest M-type dwarfs, the bright giants and supergiants, and perhaps the early-F type stars with their shallow convective envelopes (e.g., Schrijver *et al.*, 1992). The Sun moves up and down along that relationship through its activity cycle (albeit with substantial excursions from the mean), suggesting that at different phases of the cycle, its atmosphere resembles that of a star of a different level of activity. And that, in turn, suggests that the flux source function may scale with activity level from star to star as it does for the Sun with time, only with a significantly larger range.

For the active regions (i.e., for those regions that at some phase contain spots or pores), the spectrum of emerging fluxes appears to simply scale up and down by a multiplicative factor, spanning a range of about 8 (Harvey, 1993). This is the basis for the assumption that the flux spectrum can be multiplied by a constant in the extrapolation to stars.

For the smallest bipolar regions with intrinsically strong magnetic field, called ephemeral regions, the cycle amplitude is much smaller (apparently closer to 2), while for the intrinsically weak fields that cycle dependence appears to be even less (Hagenaar, private communication). Because ephemeral regions populate much of the quiet network (which contributes significantly to radiative losses from the chromosphere at all times, and even from the corona at cycle minimum), a successful model should include the full range of bipoles associated with atmospheric emission. This led to the following choice for the number $n(\Phi, \mathcal{A})\mathrm{d}\Phi$ of active regions with total, unsigned flux Φ to $\Phi + \mathrm{d}\Phi$ to emerge onto the stellar surface per unit time, given the time-dependent dynamo activity

$\mathcal{A}(t)$, with a maximum value of $\mathcal{A}_0$:

$$n(\Phi, \mathcal{A}_*(t))\mathrm{d}\Phi\mathrm{d}t = 8 \left(\frac{\mathcal{A}_*(t)}{\mathcal{A}_{\odot,0}} \Phi^{-1.9} + \left(\frac{\mathcal{A}_*(t)}{\mathcal{A}_{\odot,0}} \right)^{1/3} \Phi^{-2.9} \right) \mathrm{d}\Phi\mathrm{d}t \qquad (1)$$

(for $1.2 \times 10^{19} \leq \Phi \leq 1.5 \times 10^{22}$), where the two terms are for the active and ephemeral regions, respectively.

It is tempting to speculate that the ephemeral regions are generated by a different dynamo mechanism than the larger bipolar regions. A turbulent dynamo operating in the near-surface layers has been suggested as their source. But we have to bear in mind that ephemeral regions do vary in phase with their larger relatives (which may, of course, reflect a coupling of the large-scale and near-surface dynamos), while they also extend the butterfly wings of solar activity by a few years before and after the sunspot minima at either side of the sunspot cycle (Harvey, 1992). That is strong evidence that at least a substantial fraction of the ephemeral regions is generated by a dynamo process that is coupled to that which generates the active regions, if it is not indeed the same.

Active latitude range

Whereas we can make a plausible case that the active-region spectrum simply scales up and down with activity (while accommodating the reduced variability of the ephemeral regions), we know almost nothing empirically about emergence latitudes and spreads therein for other stars (or, for that matter, about latitudinal preferences; compare Berdygina *et al.* in these proceedings).

There are theoretical studies that show how the mean latitude of flux emergence may shift as a function of stellar type or of rotation rate and – coupled to that – activity level. The model by Granzer *et al.* (2000) suggests that for a star like the Sun, with a moderately deep convective envelope, rotation rate appears to make little difference in the emergence latitudes unless the rotation period is less than about one tenth of the current value; for shorter periods the mean latitude increases significantly, up to about 30 degrees, while a zone of avoidance near the equator may develop. For the rotation range that we study, from solar down to a rotation period of approximately 6 days, this result is compatible with our choice to adhere to the solar properties for emerging field.

2.2. Flux dispersal and removal

Not long after the discovery of the supergranulation pattern, Leighton (already in 1964) proposed that photospheric flux is subjected to a random walk within that evolving flow field. Large-scale patterns within the field, determined by the properties of the flux source, would consequently evolve as if the field were diffusing across the photosphere (this process is not to be confused with magnetic diffusion, of course).

That concept has proven to be remarkably successful over the years, as demonstrated by Sheeley, Wang, DeVore, and others (see Sheeley *et al.*, 1987, as an entry point to their work). Leighton already knew that differential rotation played an important role, but the realization that there also had to be a weak but persistent poleward meridional advection came later (postulated by Mosher in 1976, observed by Duvall in 1979, and modeled by DeVore *et al.* in 1984).

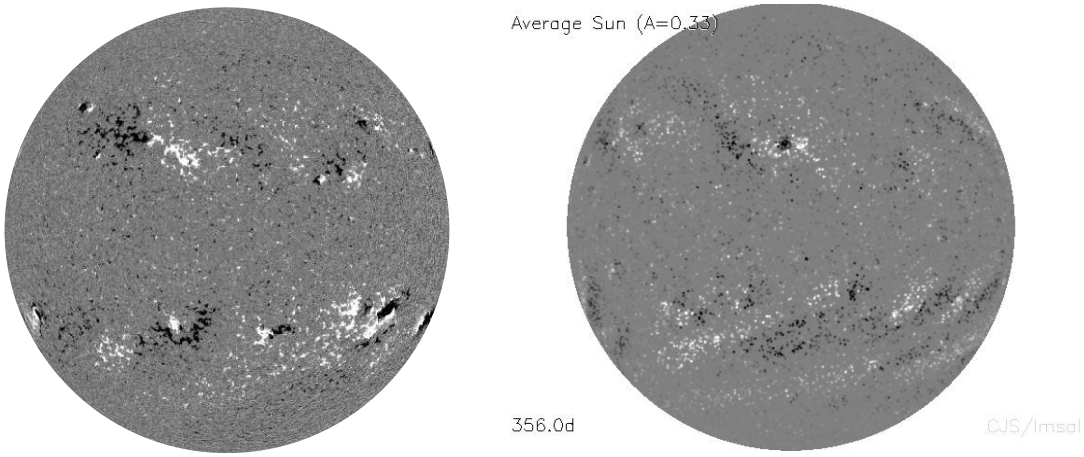

Figure 1. Left panel: Sample MDI magnetogram for 12 Jun 1998 (6:27 UT). Right panel: Sample full-disk magnetogram for the average Sun based on simulations with the standard model (Schrijver, 2001); this image resembles the solar pattern, but is not an attempt to fit the solar field. The simulated disk has been subjected to a smearing with a Gaussian with FWHM of 5,600 km, resulting in a comparable resolution as the image on the left.

Once the sources of the magnetic flux are specified, the model explains, at least to first order, the northeasterly arched unipolar (not to be taken for monopolar) regions, the location of the polar-crown filaments, and the polarity reversals of the polar caps in antiphase with the sunspot cycle. It remains to be seen whether it describes all of the features up to the large-scale dipole field of the Sun, and the associated polar caps, but its success leaves little doubt that it is a dominant process for the evolution of the large-scale solar magnetic field.

Patterns and survival times

The largest of the active regions are responsible for the large-scale patterns in the field (Sheeley, 1992), such as the unipolar poleward arcs (see Fig. 1, lefthand panel). The flux in these patterns, although weakened continually in the interaction with the surrounding regions, survives for many months, and the small fraction that reaches the polar caps survives for years. On the other hand, very few of the multitude of individual concentrations of flux within these large-scale patterns survive for very long.

Two processes severely limit the survival of any concentration. First, there is the process of fragmentation: any flux concentration is broken apart by the convective motions. This may be the dispersing of a cluster of subresolution concentrations or may truly be the breaking up "monolithic" structures; likely both processes occur. The fragments continue their random walk, and may later merge again with field of the same polarity.

The second process becomes clear when we think of the collision of two flux concentrations of opposite polarity. Although we do not understand the details of what happens, we see that in such a case the minority polarity cancels

against a matching amount of flux of the majority polarity. If this happens at the interface of two polarity patches covering a relatively large area, flux has been permanently removed from the photosphere. But if this happens between a flux concentration that can trace its history back to an active region and two nearby poles of a small (ephemeral) bipole shortly after the latter emerged, then no net flux has been injected or removed on the associated time scale of a few hours. What has happened, however, is that the canceled flux has effectively been moved to the location of the remaining pole of the ephemeral region. This process does not act diffusively on the flux. It does keep the network from collapsing into a limited set of particularly strong convective downflows in the supergranulation. It also forces continued reconnection in the outer atmosphere (and possibly is associated with that below the surface also), where it may contribute noticeably to coronal heating (see Schrijver *et al.*, 1998, and references therein).

The time scale on which all magnetic connections are broken within the quiet-Sun corona as a consequence of this process is remarkably short: within the mixed-polarity network, as much (unsigned) flux surfaces in concentrations of 10^{18} Mx or more as exists there on a time scale of ~ 0.5 d (Hagenaar, 2001), or in concentrations of 10^{19} Mx or more in ~ 2 d (Schrijver *et al.*, 1997).

The combined effect of fragmentations, collisions, and interactions with ephemeral regions results in a broad (approximately exponential) distribution of fluxes in the concentrations within the quiet Sun as well as within magnetic plages. Tracking these concentrations in the quiet Sun reveals a trend in which larger concentrations have a smaller rms displacement than smaller ones. It remains to be established whether this is a consequence of a stabilizing effect on the flows by the presence of the magnetic field, or whether larger concentrations build up more easily in the sinks of more persistent flows. The effect of this trend is that the net dispersal coefficient for flux is $2-3$ times larger than what would be estimated from tracking large concentrations only (compare Eq. 3 below).

Large-scale flows

None of the three flow fields that are involved in the dispersal of flux, i.e. the differential rotation, the meridional flow, and the supergranulation, are understood well enough to be able to predict how they vary with stellar parameters. The magnitude of the differential rotation is marginally accessible to observational scrutiny by assuming that the dispersal in rotation rates inferred from brightness modulation for a given star at different times is a consequence of active-region emergence at different preferred latitudes, and perhaps from some Doppler-imaging techniques. The surprising result of these efforts is that the differential rotation, when expressed as the time it takes for pole and equator to differ by one full rotation, shows little scatter from star to star for most of the main-sequence stars, whether single or in close binary systems. There is some evidence that this profile may be different in F-type stars with shallow convective envelopes, and in some evolved binary systems (see contributions by Hackman and Jetsu, Reiners, and Weber *et al.*, in these proceedings on the topic of differential rotation).

There is no generally accepted model for the meridional flow either. This flow likely develops in part as a consequence of anisotropic convection (e.g., Kitchatinov and Rüdiger, 1995). It has been observed to persist over at least

$\sim 20,000$ km in depth using helioseismic techniques (e.g. Basu *et al.*, 1999; González Hernández *et al.*, 1999), which at present allow for quite a range in magnitude and extent of the flow.

It is remarkable that in the half century since its discovery, the cause of the supergranulation is still not understood; concepts for its origin range from early ideas that it was a consequence of the ionization of helium to the more recent notion that it is but part of a continuous spectrum of convection, of which granulation, mesogranulation, and supergranulation are all part. The very strong stratification in the outermost layers of the solar convection zone has until now precluded modeling of convection over the depth range that is required to study granulation and supergranulation with the same detail, or to span the depth of the convection zone from the bottom to the layers that encompass most of the supergranulation. Even observationally the determination of the entire spectrum of convection is difficult, because the different scales show up most clearly in different diagnostics (intensity images, divergence maps, and time-averaged Doppler maps or the chromospheric network, respectively; e.g. Hathaway *et al.*, 2000). Within the context of our model, this means that we must rely on our knowledge of solar supergranulation, differential rotation, and meridional flow; the study of the dependence of activity on supergranular properties (compare contributions by Freytag and by Gray in these proceedings) and on the coupling between field and flow at activity levels not seen on the Sun, for example, must await future theoretical work.

2.3. Activity, field patterns, and polar activity

Combination of the flux-emergence statistics and the model for field dispersal allows us to simulate the surface field. An example is shown in the righthand panel of Fig. 1. This compares well with the general appearance of actual solar magnetograms (such as in the lefthand panel; note that the similarity is by chance, as the model is not used at present to simulate the actual solar field). The model not only compares well in terms of the patterns, but reproduces both the total amounts of flux on the surface and the histograms of observed flux densities very well.

For one thing, the model can be used to calibrate the flux injection rate $\langle E_* \rangle$ (Mx/s) against the associated average unsigned surface flux Φ_* (Mx) in the stellar photosphere (Fig. 2):

$$\frac{\langle \Phi_* \rangle}{10^{24}} = 0.8 \left(\frac{\langle E_* \rangle}{10^{18}} \right)^{1.01 \pm 0.01} . \tag{2}$$

Deviations from this relationship do not exceed a factor of two for the flux-injection parameter (equivalent to active-region emergence rates) $\mathcal{A}$ ranging from 10^{-5} to 10^{2}, and average surface fluxes ranging over a factor of ~ 500.

The fact that the flux-balance relationship in Eq. (2) is close to linear is remarkable. This can be understood as follows. In the domain of very low activity labeled "A" in Fig. 2, the few bipolar regions evolve largely independently of each other, resulting in a linear relationship. In the low-activity domain "B" and in the high-activity domain "D," one of the two power-law terms in the flux-input spectrum of Eq. (1) dominates, somehow resulting in a power-law index ~ 0.7. Only in the domain "C" of intermediate activity, which contains the Sun

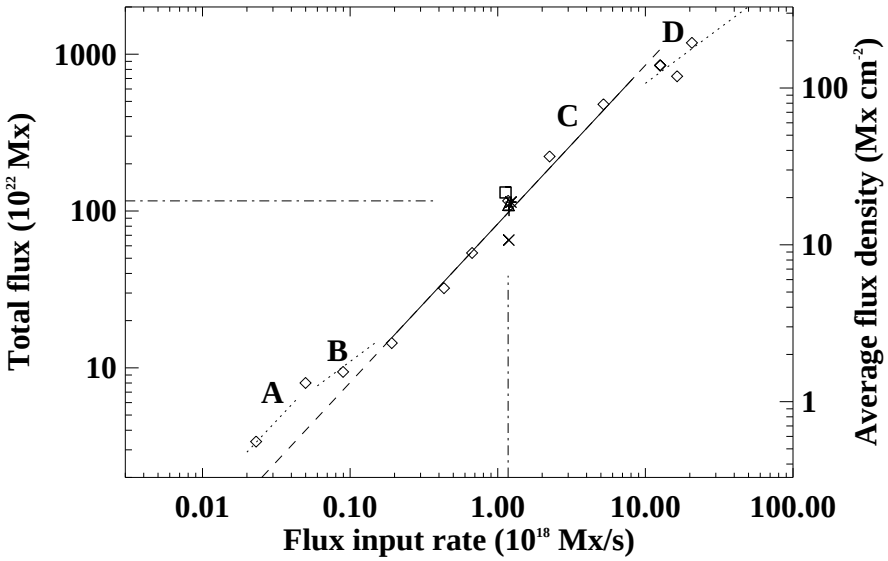

Figure 2. Model results for the dependence of the total absolute flux (left-hand axis, for latitudes below 60°) or the surface-averaged absolute flux density (right-hand axis) on the rate of flux injection into a stellar photosphere. The diamonds represent the results from a set of standard model runs; the dashed-dotted line segments identify the standard model for the active Sun. The power-law fit (solid line) to the range between 0.2 and 5 times the rate of flux input for an average Sun has a slope of 1.0. Other runs for an active Sun, but with zero meridional flow or 10 times the solar meridional flow, and for a flux-independent flux-dispersal coefficient of 200 km^2/s nearly coincide with the standard-model run for the active Sun. The square shows the result of a simulation with zero differential rotation; the cross is for a flux-independent flux-dispersal coefficient of 600 km^2/s.

throughout the cycle, does the source-spectrum change occur in such a way as to result in a linear relationship. We can at present only wonder whether the linearity of the relationship is necessarily how a dynamo regulates its flux budget, or whether it is simply by chance that the function $\langle \Phi_* \rangle$ is linearly dependent of $\langle E_* \rangle$ for a star like the Sun.

The dispersal of magnetic flux in the combined flows associated with supergranulation, differential rotation, and meridional flow results in poleward streaks of flux of largely one polarity (compare the sample real and model magnetograms in Fig. 1, and the cycle summaries in Fig. 3). Within the ensemble of these unipolar arches, net flux of the following polarity is transported to the poles because of the way active regions emerge: the leading polarity tends to come up somewhat closer to the equator than following polarity (Joy's rule), which means that leading polarity has a slightly larger probability to cancel across the equator, leaving a relatively small excess trailing polarity to reach the corresponding pole (this would happen even in case there were no meridional flow, but the slope in the unipolar arches would then be different). Note that

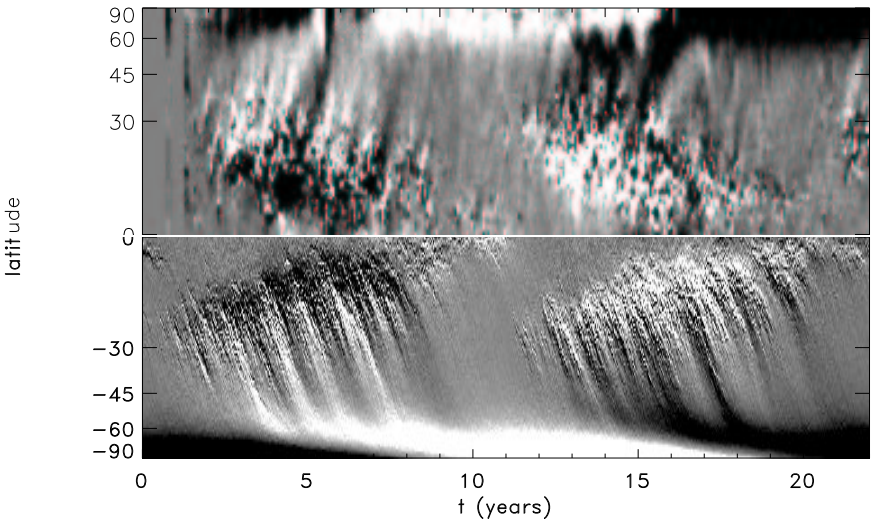

Figure 3. Comparison of synoptic charts. The upper half of the figure shows as a function of time, the longitudinally-averaged net flux against latitude for the period 1976-1998. The lower part shows the result of a simulation. Note that the simulation results are much less noisy, largely because information on the full sphere is averaged, while for the top half so-called synoptic data are used, which are a weighted average of only the flux near the central meridian. N.B. The sign of the polarity in the solar data was changed to match that in the simulation. (Modified after Schrijver and Title, 2001).

there are strong fluctuations on this tendency: Fig. 3 shows that some poleward streaks of the leading polarity also occur, both in the observations and in the simulations.

The result of this transport is that over time an excess of trailing polarity builds up to form unipolar areas over the solar rotational poles (Fig. 3, and the lefthand column in Fig. 4). As the next polarity cycle begins, net flux of the opposite polarity is transported to the poles, which eats away the existing polar cap, after which a new cap of opposite polarity begins to form. The cycle variation of the polar caps is essentially in antiphase with the sunspot cycle.

If the flux transport were a linear process (as in the earlier Sheeley and Wang model), an increase in cycle amplitude by a certain factor – and not changing any of the other flux emergence properties – would be matched by the change in the flux in the polar caps. If, as discussed in Section 2.1, the dispersal process is nonlinear, the field pattern depends on the activity level: as more flux emerges onto the stellar surface, the polar flux coagulates into larger concentrations because of the increase in the collision frequency within the more densely packed environment. Because these larger concentrations are less mobile than smaller concentrations, the random-walk dispersal of polar flux against the concentrating meridional flow is less effective, and the flux is concentrated into a narrower polar cap (Fig. 4). The simulations show that instead of a polar cap of a single polarity, a pattern develops in which the polar cap is encircled by

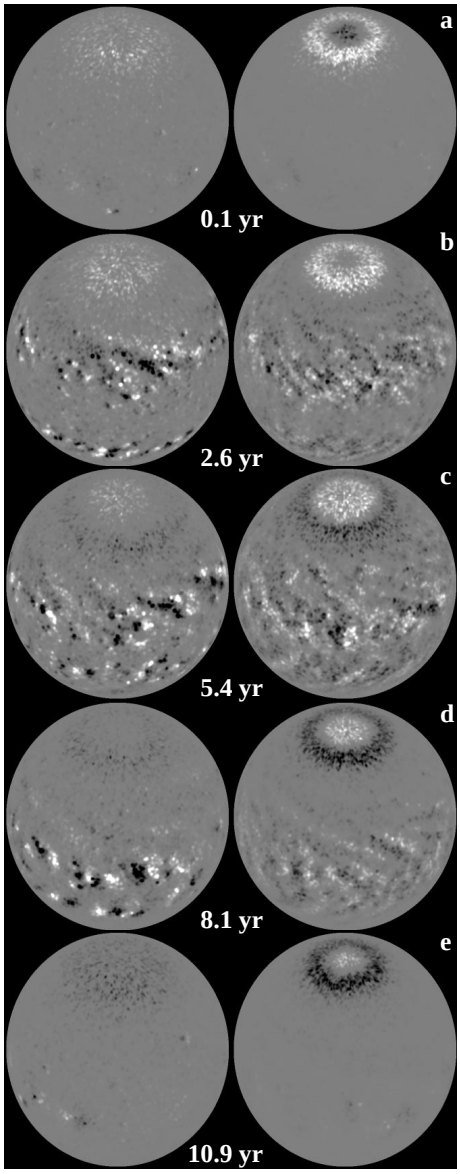

Figure 4. Simulations of stellar magnetic fields for a star like the Sun (left) and for a star with an active-region emergence rate 30 times higher (right). The panels show the surface magnetic field, viewed from a position over a latitude of 40°. The gray scale for the Sun-like star saturates at $70\,\mathrm{Mx\ cm^{-2}}$, and for the active star at $700\,\mathrm{Mx\ cm^{-2}}$, for a resolution of one square degree. The flux density has been multiplied with a projection factor of $\cos(\mu)$, with μ the angular distance to the center of the disk, to simulate the weakening of the signal towards the limb for a field that is normal to the surface.

a ring of opposite polarity. The longitude-averaged flux density is predicted to reach $300 - 500\,\mathrm{Mx\,cm^{-2}}$ for a star with a rotation period of approximately 6 d. For more active stars, or for stars with longer cycles, even higher flux densities are to be expected.

The pattern change from a single-polarity polar cap to a bipolar core-ring geometry can be understood quantitatively by estimating the time scales involved. The effective diffusion coefficient for flux in a unipolar environment with an average (unsigned) flux density φ is (according to paper II) approximately

$$D^*(\varphi) \approx \frac{900}{\left(1 + 0.27\sqrt{\varphi}\right)^2}\ \ (\mathrm{km^2/s}) \tag{3}$$

(which is approximately linear in φ for values exceeding a few hundred Mx cm^{-2}). The time scale for flux to be diffusively transported from $\sim 70^\circ$ to the poles, i.e. over a distance $L = 0.35 R_\odot$, is of order

$$\tau_{\theta=70} \sim \frac{L^2}{4D^*} \sim 0.5\,(1 + 0.27\sqrt{\varphi})^2 \quad \mathrm{yr}. \tag{4}$$

For the Sun, with a polar-cap flux density φ of order 5 Mx cm^{-2}, we find that $\tau_{\theta=70} \sim 1.4$ yr, which is significantly shorter than the cycle duration; the entire polar cap therefore changes sign in antiphase with the cycle. For a tenfold increase of the active-region emergence rate $\mathcal{A}_0$, φ near the poles is of order $50 - 100$ Mx cm^{-2}, so that $\tau_{\theta=70} \sim 4 - 7$ yr. For a thirtyfold increase, $\varphi \sim 150 - 350$ Mx cm^{-2}, and $\tau_{\theta=70} \sim 9 - 18$ yr. Consequently, on a very active star with ($\mathcal{A}_{*,0} \gtrsim 20$), an 11-year sunspot cycle is already well on its way to create a high-latitude ring of trailing-polarity flux well before the polar cap has disappeared, creating the two-polarity pattern as in the right-hand column in Figure 4. Note that the result of the slowed diffusion on an active star is that the simulations exhibit a strongly reduced variation in the total flux in the polar caps above a latitude of 60° compared to the solar case. For the Sun-like star, the amplitude in the flux poleward of 60° is a factor of ~ 3.4 through the sunspot cycle. For $\mathcal{A}_{*,0} = 10$, the amplitude is reduced to a factor of ~ 1.5; for $\mathcal{A}_{*,0} = 30$, it is a mere factor of ~ 1.25.

The high flux densities that are expected within the polar caps of active stars are, at moderate angular resolution, found on the Sun only in regions of spots and in dense pore clusters. We do not know, at present, whether the concentration of such amounts of flux by large-scale advecting flows can lead to a collapse of bright faculae into dark pore and spot clusters. On the Sun, spots only form immediately upon emergence of flux, while there are only very few reports that pores form by the chance coagulation of flux well after emergence. But then again, there is no environment like these polar caps on the Sun: mature plages have an average flux density of the order of $100 - 150$ Mx cm^{-2}, i.e. only 1/5 to 1/2 of the average polar-cap value for the moderately active star with $\mathcal{A}_{*,0} = 30$.

If flux can indeed coagulate to form spots and pores when packed close together, the consequence is a natural formation of polar starspots. Starspots at high latitudes, or even truly covering the stellar rotational poles, are common among the most active of the cool stars. The overview by Strassmeier (2000) shows that of the 53 stellar systems (including 6 pairs of individually imaged stars in close binaries) for which Doppler images were available in 1999, 32 ($\sim 60\%$) have polar spots. All but two of the 53 stellar systems have high-latitude, if not truly polar spots. Whereas most of the stars with truly polar spots are very active, tidally interacting RS CVn type binaries, it is not binarity that is crucial to the formation of a polar spot: the sample also includes 11 young T Tauri stars, 3 single FK Comae stars (rapidly-rotating, single, cool giants), 4 W UMa contact systems and young, rapidly rotating main-sequence stars. For one case (HR 1099), Vogt *et al.* (1999) claim that they observe spots that form at low latitudes, and that then move poleward in what appears to be a meridional flow at 6-30 m s^{-1}, to eventually merge with the polar spot.

The advection of a preponderance of one polarity to the pole is such a natural consequence of the injection of tilted bipoles into a stellar photosphere,

that it is hard to see how it could not contribute significantly to the polar cap fields in cool stars. It is likely that a second process works in addition to this: the Coriolis force that acts on magnetic flux bundles rising from deep within the star is likely to deflect flux poleward, increasingly so as we look at stars with decreasing rotation periods. Schüssler *et al.* (1996), Buzasi (1997), and Deluca *et al.* (1997) argue that this force deflects rising flux toward higher latitudes, although probably no higher than 60° (see also the study by Granzer *et al.*, 2000). Schüssler *et al.* (1996) speculate that truly polar spots could result from a flux eruption originating very deep in stars with relatively small radiative interiors, or – in stars with a relatively shallower convective envelope – by a poleward slip across the radiative core of segments of flux rings.

2.4. The outer-atmospheric field

The photospheric sources form the main contribution to the outer-atmospheric magnetic field, in addition to which there are electrical currents within the atmosphere and passing through the stellar surface. Without these currents, the field would be purely potential. The observed solar field deviates significantly from potential in the vicinity of filaments and on the largest scales for the outer-coronal or inner-asterospheric field. Within active regions, however, a potential-field extrapolation is generally an acceptable approximation (e.g., Lee *et al.*, 1999, and references therein), particularly when studying the general appearance of the field rather than the detailed connectivity.

Snapshots of the potential field configurations for the three simulated stars (with peak active-region emergence rates $\mathcal{A}_{*,0}/\mathcal{A}_{\odot,0} = 1, 10, 30$) are shown in Fig. 5. At phases near cycle minimum (top and bottom rows), the coronal field is dominated by the large-scale dipole field. For the Sun, some low-latitude fields over (remnant) near-equatorial active regions also show up, but the much stronger polar-cap fields on the active stars make their active-region component under-sampled in the display. Near cycle maximum, the polar-field configuration in active stars is such that the two nested opposite-polarity rings at high latitudes are of comparable flux, so that the large-scale dipole field is relatively weak compared to the cycle-minimum phases and the associated field lines rare. The global dipole and quadrupole components for the active star are of significant strength even in these phases, however, as can be seen from the fact that even the lower-latitude field lines often show a preferential alignment with the north-south direction, particularly for the higher-arching loops. The dense packing of active regions, and the nesting of successive generations of active regions, on such an active star not only makes it impossible to determine unambiguously which patch of one polarity emerged with what of the opposite polarity on a single magnetogram, but also the potential-field loops often do not connect the polarities that emerged together within a bipolar region.

Note that the polar arcade that connects the polar cap to the ring of opposite-polarity flux may well be a location of massive filaments and/or flares and mass ejections as the fields are sheared out of the potential state.

The run of field strength with height along loops exhibits substantial diversity, of course. On average, the characteristic height over which the field strength reaches 1/e of the base field strength within regions where the flux

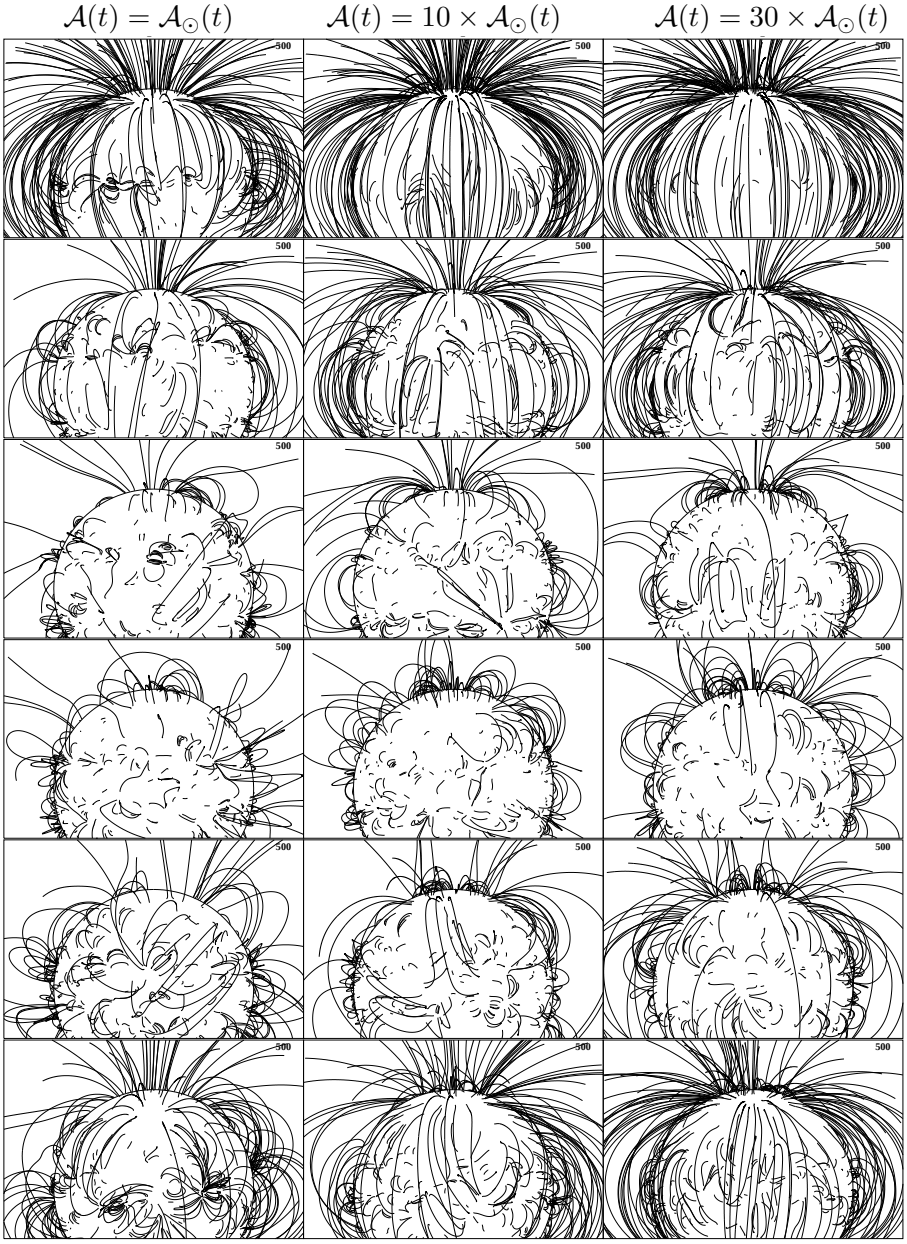

Figure 5. Potential field geometry of stellar coronae. Each of the panels shows 500 randomly selected field lines (including in that total field lines behind the sphere). The columns show a star of solar activity, and stars with 10 and 30 times the solar active-region emergence rate, respectively, in six different phases of the 11-year starspot cycles: 0.00 (top, cycle minimum), 0.16, 0.33, 0.49 (near cycle maximum), 0.65, and 0.82 (bottom); sample magnetograms for these phases for the simulations of the Sun-like star and of the most active star are shown in Fig. 4. The field line density within each panel is statistically proportional to field strength.

density exceeds 50 gauss on a Sun-like star is ~ 15 Mm; for $\mathcal{A}_{*,0} = 30$, that value is $30 - 40$ Mm.

2.5. Non-radiative heating and flux-flux relationships

One of the most remarkable properties of stellar outer atmospheres was already referred to in Section 2.1: if stellar radiative flux densities $F_{\rm i}$ in individual spectral lines, or in appropriate spectral pass bands, originating from within the outer atmospheres are compared, these disk-averaged emissions define power laws that extend over more than four orders of magnitude in soft X-rays (first pointed out by Ayres *et al.*, 1981; Zwaan, 1981; Oranje *et al.*, 1982), regardless of the stellar mass, surface gravity, or effective temperature, at least from mid-F to mid-M type stars from the main-sequence up to bright giants. The observed power-law indices range over a factor of two up and down from unity, depending on which two diagnostics are compared.

The nonlinear relative scaling of most radiative flux densities rules out that a stellar outer atmosphere is composed merely of some fixed ensemble of building blocks for which only the frequency differs for stars of different activity. With the model thus far discussed, the distributions of magnetic field on the simulated stellar surfaces can be combined with the associated expected radiative losses from the atmosphere to compute surface-averaged losses expected from them as point sources. The simulations of the surface magnetic field discussed in Section 2.3 have demonstrated that power-law relationships then occur naturally as the disk-integrated counterparts of the relationships that are found when observing the Sun with moderate angular resolution (large enough to average over a sufficiently large set of individual structures, but small compared to the Sun's surface area). Starting with the power laws observed for the spatially-resolved Sun, the expected relationships between disk-averaged magnetic and radiative diagnostics have power-law indices that lie within $10 - 15\%$ of the values for the local relationships.

The transformation from local to global radiative losses is straightforward as long as there is a good local correspondence between the photospheric magnetic flux density and the atmospheric radiative losses, as is true, for example, for chromospheric emissions. But this condition is not met within the corona where loops extend over long distances while their geometry depends on the ensemble of all field sources. If we desire, moreover, to study the distribution of plasma temperatures and densities in the corona, the coronal part of the outer stellar atmosphere needs to be studied in some detail.

Loop atmospheres

Coronal loop atmospheres have often been approximated using a model developed by Rosner *et al.* (1978), generally referred to as the RTV model, based on the assumptions that loops are quasi-static, isobaric, uniformly heated, and of constant cross section. We have had to realize that at least three of the four assumptions cannot be used for general loop modeling:

Loop cross sections present us with a particularly baffling problem. The magnetic field of active regions is expected to decrease with increasing height as the field lines fan out leading away from the photospheric sources. On average this must be true, because the area of the projection of the bright active-region

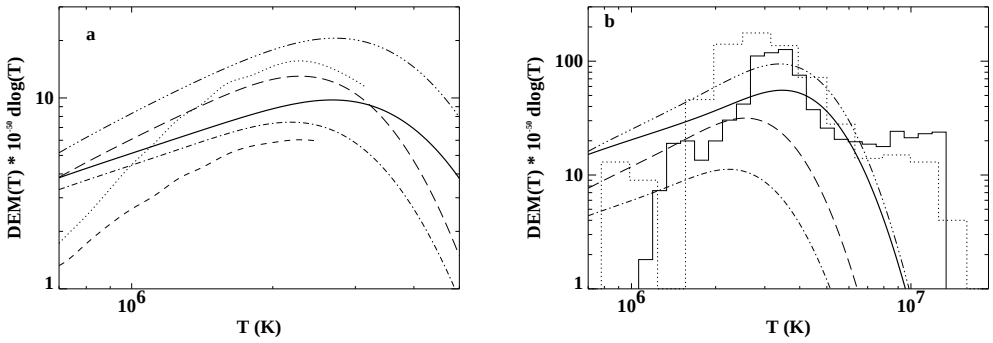

Figure 6. *a*) Differential emission measure curves for the Sun, short-dashed for the high-FIP and dotted for the low-FIP elements (see paper III for a detailed description, data from Laming *et al.*, 1995, and the simulation results for cases with $\beta = 1$ or 1.4, $\lambda = 0.5$ or 1, $\nu = 0$ or 1, and $s_{\rm H} = 20\,{\rm Mm}$ (long-dashed and dashed-triple-dotted) or $s_{\rm H} = \infty$ (dashed and dotted). *b*) As *a* but for χ^1 Ori (dotted histogram) and ξ Boo A (solid histogram), and for a model star with $\mathcal{A}_{*,0} = 30$.

corona is always larger than the plage area on the photospheric magnetogram (compare, for example, *MDI* and *EIT* images on *http://www.maj.com/sun/*). Consequently, one expects coronal loops to show the same average ratio for the expansion between the low segments (not considering the part below the chromosphere here) and top parts. Surprisingly, however, several studies have found that loop diameters appear to be nearly constant along their entire coronal segment for $3-5\,{\rm MK}$ X-ray loops as observed with *YOHKOH/SXT* (Klimchuk, 2000) as well as for $1-2\,{\rm MK}$ (quiescent and post-flare) loops observed with *TRACE* (Watko and Klimchuk, 2000). In both of the above studies there are loop diameters that average significantly above the instrumental resolution (the average diameters are 10,000 km and $\sim 4,000\,{\rm km}$, respectively). Yet, the average expansion for the coronal segments of the loops appears to be less than 30%.

Recently, Aschwanden *et al.* (2000, 2001) have argued that many solar coronal EUV-bright loops are incompatible with the traditional RTV model: observed loops appear to be far more isothermal than predicted by the RTV model. They also find that many of the loops are not stratified in accordance with a hydrostatic approximation; it remains unclear whether the observable set of loops is dominated by dynamically evolving loops, thus biasing the sample, or whether indeed most of the EUV-bright loops are incompatible with hydrostatic stratification. Aschwanden *et al.* (2001) do find that at least a fraction of the loops can be described by a quasi-static model, provided that the RTV assumption of uniform heating is relaxed: if loops are heated primarily – though not exclusively – in the lower 10-20 Mm above their base, then the quasi-static approximation, with plasma stratified under the influence of gravity, at least still holds for a significant fraction of the loops. MacKay *et al.* (2000) study hotter (3-5 MK) loops observed by *YOHKOH/SXT*; they also find a best fit for base-dominated heating, even though other heating profiles appear to be

allowed within the uncertainties. It may thus well turn out that most of the solar coronal heating in non-flaring conditions occurs in the lower 10-20 Mm of the corona (which is, interestingly, comparable to the scale height of the coronal field over active regions; see the end of Section 2.4).

Until better understanding of the statistics and physics of coronal loops is formulated, we are left with little alternative but to use the modified RTV loops with a stratified heating, as developed by Serio *et al.* (1981). In order to compute the radiative losses of entire coronae, we do not model each field-line atmosphere separately. Instead, we approximate the loop atmospheres by an analytical expression for the run of temperature along a loop, that is based on a sample of model loops of a range of lengths and heating scale lengths.

We compute loop atmospheres only for (1) loops with apex heights above 4,000 km over the top of the chromosphere and apex heights below a solar radius (thus excluding what in a real field configuration would mostly show up as coronal holes), (2) loops for which the field strength at either chromospheric loop base is less than 1,000 gauss (reflecting the fact that on the Sun loops anchored in sunspots are X-ray dark; e.g. Sheeley *et al.*, 1975), and (3) loops for which density decreases monotonically with height (long loops that are long relative to the heating scale length show density inversions, which likely destabilizes them).

Heating the loop atmosphere

Given a field geometry and the basic model for a loop atmosphere, one needs to know how much energy is available to heat each loop volume. We parameterize the flux density $P_{\rm H}$ (erg cm^{-2} s^{-1}) through the base of the loop as a product of power laws of the field strength at the coronal base (power-law index β), the length of the loop (index λ), and the velocity with which the field is being moved about (index ν). We explore a range for the parameter β that spans essentially that found in the literature (see the compilation by Mandrini *et al.*, 2000), i.e. -1 to 2. The range for λ (from -2 to 2) is extended to somewhat higher values than found in these models because the simulations show that solar constraints in principle allow such values. For ν we explore the range from 0 to 2. Note that we ignore any dependence on density because most such dependences are relatively weak. The values of other parameters, such as the Reynolds number, would have to follow from detailed modeling, which was beyond the scope of the study.

For the velocity, we use a parameterization that reflects the fact that the rms dispersal coefficient in a plage environment at ~ 100 gauss is a factor of 1.6 lower than in the quiet network (Schrijver and Martin, 1990). If we take that effect to be a consequence of a change in velocity, then we can use an exponential approximation,

$$v = 0.4 \exp(-|\varphi|/220)\,({\rm m/s}), \qquad (5)$$

at an absolute magnetic flux density $|\varphi|$ as measured at moderate resolution.

Once all computed coronal loops are populated with an atmosphere, the expected differential emission measure distribution, $DEM(T)$, for the entire corona can be computed. From that, radiative losses for a soft X-ray pass band (like that of *EINSTEIN*, *EXOSAT*, and *ROSAT*) are estimated based on the model published by Mewe *et al.* (1985, 1986), with photospheric abundances as published by Meyer (1985). The latter allows comparison with results published

in the older literature, but of course ignores the abundance differences between active and inactive stars (see, for example, contributions by Audard, Dupree, Güdel, Huenemoerder, Linsky, Raassen, and Osten in these proceedings).

In paper III, we find the following best-fit parameterization for the heating flux density $P_{\rm H}$ (erg cm^{-2} s^{-1}) in quiescent conditions:

$$P_{\rm H} \approx P_0(s_{\rm H})(B_{\rm base}/100)^{1.0\pm0.5}(\ell/24)^{-0.7\pm0.3}(v/0.4)^{0.0\pm0.5}, \qquad (6)$$

for base field strength $B_{\rm base}$ (gauss), loop half length ℓ (Mm), and foot point velocity v (km/s); the uncertainties in the exponents reflect the allowed range. The constant of proportionality, $P_0(s_{\rm H} = 20\,{\rm Mm}) \approx 2.0 \times 10^7$ or $P_0(s_{\rm H} = \infty) \approx 1.5 \times 10^7$ erg cm^{-2} s^{-1}, ensure an apex temperature of 3 MK for a loop with a foot point separation of 30,000 km, characteristic of active-region loops (e.g., Golub and Pasachoff, 1997).

The above expression for the coronal heating flux density is, of course, the result of a fit to a set of solar and stellar constraints. It is therefore not truly a parameterization of solar observations applied to stars, as was the case for extrapolations in the preceding sections. Yet it can be seen as such, because paper III points out that much the same fit would have been found if it had been based only on the solar constraints (both for the star as a whole and for detailed observations of entire active regions – see Fludra and Ireland in these proceedings – or of individual loops – as observed by Mandrini *et al.*, 2000). That fit also matched total soft X-ray flux densities from cool stars as well as the characteristic coronal temperatures of stars of a range of activity levels.

The above best-fit expression favors coronal heating mechanisms that rely on the driving of current layers or turbulence, with either low- or high-frequency driving, or perhaps both (see paper III for a detailed discussion).

The best-fit parameterization of the coronal heating is rather insensitive to the driving velocity, or that the driving velocity is insensitive to the base field strength. This may, at first sight, seem surprising, particularly because observations suggest that the dispersal rate of larger concentrations is reduced relative to that of smaller ones. But that difference in the rms displacements on long time scales does not appear to hold for the instantaneous velocities that may be involved in coronal heating. Berger *et al.* (1998), for example, use an image set with a cadence of half a minute to measure the velocity distribution of G-band bright points (which are tracers of a subset of the magnetic flux concentrations). These are found to have an average velocity of 1.1 km/s in quiet Sun and only a marginally lower value of 0.95 km/s in dense network where the field is strong enough to result in abnormal granulation. A similar result is found for significantly longer time scales that probably lie above the time scales involved in heating: using magnetograms with a spacing of approximately 2 hours, Schrijver and Martin (1990) find that the velocity distribution based on pairs of magnetograms shows no significant difference between quiet Sun and magnetic plage, even though the longer-term rms dispersal rates differ by a factor of ~ 2.

In view of this, we propose that the reduced long-term mobility of flux in magnetic plages relative to less active environments is of little consequence to coronal heating. In contrast, the short-term displacements that are likely involved in coronal heating appear to have at most a weak dependence on the

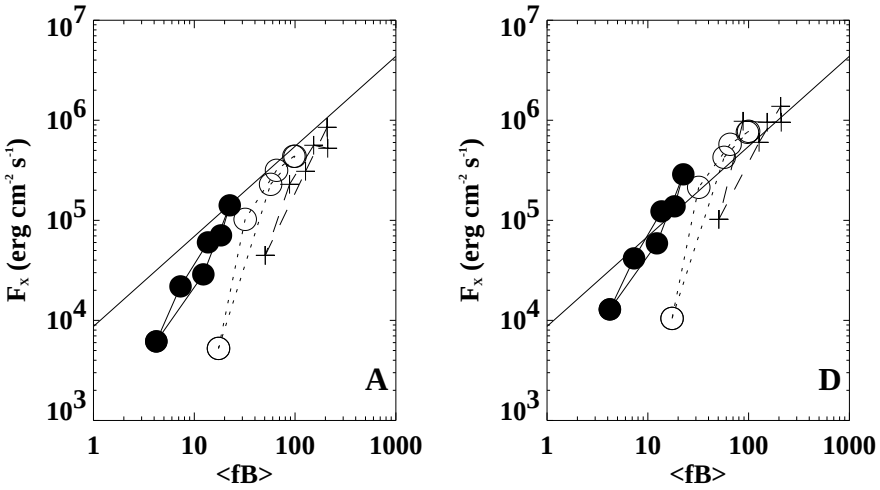

Figure 7. Soft X-ray (6-60Å) flux densities normalized to values at the stellar surface predicted by the model versus the corresponding surface-averaged magnetic flux densities, $\langle fB \rangle$ (the product of surface filling factor and intrinsic photospheric field strength), for $(\beta, \lambda, \nu, s_{\rm H}) = (1, 1, 0, \infty)$ (label A; compare solid lines in Fig. 7) and (1,0.5,0,20 Mm) (label D; compare dashed-triple-dotted line i Fig. 7). models A through F. Symbols: filled circles, star like the Sun; open circles, star with $\mathcal{A}_{*,0} = 10\mathcal{A}_{\odot,0}$; +, star with $\mathcal{A}_{*,0} = 30\mathcal{A}_{\odot,0}$. The relationship derived from solar and stellar observations is shown as a solid line (see paper III); the empirical relationship derived by Saar (2001) lies close to this line.

average local flux density. The latter is, by the way, also supported by the fact that even in dense magnetic plages where the granulation pattern differs clearly from that in non-magnetic regions, essentially the same average bolometric intensity is measured, requiring that the same amount of energy is transported to the surface per unit time. It may therefore well be that the sub–surface convective motions that drive the short-term surface displacements are affected little.

The simulations moreover suggest that essentially all loops are heated according to the above function, obviating the need for a strong selection criterion that determines which loops are heated; instead, the loop-dominated structure of the corona appears to reflect a dependence on, in particular, the value of $B_{\rm base}$ at or near the loop base.

The modeling revealed that the best-fit parameterization based on global coronal properties is rather insensitive to the heating scale length. Modeling of individual loops, on the other hand, does point out the need for a relatively short heating scale length. It is interesting to note that the length scale of $s_{\rm H} \sim 20$ Mm, that was found to apply to many solar coronal loops, is comparable to the characteristic scale height of ~ 15 Mm for the magnetic flux density over active regions on the Sun, or the equivalent number of ~ 24 Mm if it is expressed

as a scale length along a semi-circular loop. This correspondence may explain the relatively low heating scale length that was found for solar loops: energy may be dissipated primarily there where the field is strongest.

3. Limits of the Model, and Lacunae in our Knowledge

If we look back at the modeling discussed here (compare other contributions in these proceedings by Hussain and by Jardine *et al.*), we see that the list of processes that need to be (better) understood in order to simulate merely the chain of processes discussed here in some detail includes

1. Related to the dynamo:
   (a) the cycle's duration, time profile, and the likely overlap between successive cycles as it is observed to occur on the Sun,
   (b) the bipole spectrum as a function of cycle phase,
   (c) the rotation-rate dependence of the mean latitude of flux emergence and the spread about it, as well as the the tilt angles of the emerging bipoles,
   (d) the phenomenon of active-region nesting.
2. Related to flux-tube physics:
   (a) the processes of fragmentation and coagulation of flux concentrations, including the possibility to form pores and spots by collision.
3. Related to magneto-convection and other, large-scale flows:
   (a) the supergranulation and other convective flows contributing to field dispersal and atmospheric heating,
   (b) the differential rotation, and possible torsional oscillations superimposed on it,
   (c) the meridional flow, and other flows on scales comparable to the stellar size, which need not be axisymmetric,
   (d) the influence of currents on the coronal geometry.
4. Related to coronal physics:
   (a) the change in cross section along a coronal loop,
   (b) the effects of time-dependence of coronal heating on the atmospheric properties, flows along loops, and the interface with the dynamic chromosphere,
   (c) effects of abundance variations, and all microscopic physics.

The model works rather well with the assumptions that all of the above properties are as measured or inferred for the Sun. This is, however, likely to be an oversimplification. For example, the simulations of flux emergence (as by, e.g., Granzer *et al.*, 2000) show that flux is likely to emerge at higher latitudes for increasing rotation rate and increasing depth of the convective envelope. This reduces the difference in probabilities for the leading and following polarities to reach the poles. The Coriolis force that deflects rising flux poleward in this model, likely also torques the rising flux bundle more in rapid rotators than in the solar case. This increases the tilt angle of emerging flux, which in turn

increases the probability for trailing flux to reach the poles relative to that for the leading polarity. The effects of rotation are not limited to deflecting rising flux bundles. The meridional flow – which also plays a part in determining large-scale flux transport – is also likely to be affected, because it appears to be a consequence of anisotropic convection in a rotating star, counteracted in part by the rotationally–induced oblateness of the star. We are only beginning to model what the resulting meridional circulation would be.

The above list contains processes of which we know to some extent what the physics involved is. Let me address one example in which we are puzzled at an even more fundamental level, i.e., where we have ideas but too few facts to support or refute these. This has to do with the coronal temperature distribution. As discussed above, the net radiative losses and the dominant temperature are modeled quite well. In contrast, significant problems remain for the temperatures well away from those that dominate the radiative losses of a corona like that of the Sun. In particular, the coronal temperature structure is not adequately modeled around temperatures well below the peak of the $DEM(T)$. Figure 6*a* compares the derived $DEM(T)$ curve for a Sun-like star to that observed for the Sun-as-a-star around the maximum in the cycle. For the best-fit models discussed in Section 2.5, the values near the peak agree rather well with observations (as expected from the agreement of the overall soft X-ray fluxes discussed above). Towards lower temperatures, however, the observed and model curves increasingly diverge. This problem is not limited to the solar corona: a similar difference is seen in Fig. 6*b* which compares results for the stars χ^1 Ori (G0 V, $P \sim 5.5$ d) and ξ Boo A (G8V+K4V; $P_{\rm primary} \sim 6.4$ d) to our simulations.

The unexplained steepness of the $DEM(T)$ below the maximum is a long-standing problem for stellar coronal observations (e.g., Schrijver *et al.*, 1989; Van den Oord *et al.*, 1997). It has been demonstrated that no combination of quasi-steady, uniformly-heated loops of constant cross section can explain the slope of $DEM(T)$ between, say, 1 MK and about 3 MK. One proposed explanation for the difference between model and observation involves the expansion of loops with height. Such an expansion was ignored in our simulations because it appears to be incompatible with the solar observations that form the foundation of our modeling. We now find that a low heating scale length in coronal loops steepens the $DEM(T)$, but the effect is not strong enough to explain stellar curves.

An additional argument to be used in this discussion is that much of the emission around $1-2$ MK in active regions originates from the first, say, 6,000 km above the photosphere (see the examples of what is now referred to as the transition-region "moss" in *TRACE* images in, e.g., Berger *et al.*, 1999, and Fletcher and De Pontieu, 1999). Chromospheric mottles and spicules cause significant extinction of that transition-region emission away from disk center (causing, in fact, the reticulated brightness pattern that earned the moss its name). A rough estimate suggests that perhaps as much as 60% of that emission may be lost in a homogeneously covered star (comparable to a star with $\mathcal{A}_{*,0} = 30$), or even 35% for a homogeneously filled activity belt extending up to a latitude of 30 degrees on both hemispheres, as in a star of moderate activity (based on limb-brightening data from De Pontieu, 2001, private communication). For the Sun, however, the effect is probably limited to no more than 10%, leaving the steepness of the $DEM(T)$ an unsolved problem.

When we look at the $DEM(T)$ for the most active stars above about 5 MK, a significant component is seen that is not found in the modeling of a quiescent, potential-field corona. This hot component has no counterpart in the quiescent solar corona, where significant amounts of plasma at such temperatures are seen only during flares. Does this mean that that hot component in coronae of active stars is flare related? If that is case, the fact that it is persistent in these coronae suggests that a substantial number of small flares is involved (relative to the disk-integrated signal, not necessarily small compared to solar flares, of course). The finding that electron densities at these temperatures are 100 to 1,000 times the solar coronal value – as pointed out by Dupree in these proceedings – requires a relatively small filling factor for this hot plasma. How is this to be reconciled with the requirement that the time variability should not be too strong? Many smallish flares all over the star as a consequence of the high rate of flux emergence? This is clearly where the solar analogy exceeds its limits, and stellar observations are teaching us something new, although we are not certain at present just what we are encountering.

4. Needs for the Future

The focus of this 12th workshop was on the future of the study of cool stars, stellar systems, and the Sun. The fidelity of our modeling continues to increase significantly, we have seen major additions to our empirical knowledge, and have revised our thinking about solar and stellar magnetic activity. Where, now, lie our future needs? Where are the most significant gaps in our knowledge? Where can we expect the most significant advances? Where do we need them? Among the most important areas that need to be addressed, we find the dynamo and (magneto-)convection, the dynamics of a non-vacuum magnetic field (involving reconnection, waves, etc.), energy dissipation and the resulting heating, details of field-matter interaction (including radiation and chemistry – such as for CO), and access to empirical diagnostics for the plasma microphysics.

Each of the subareas in our field will of course benefit from advances in modeling and instrumentation. A new realization, however, is that it seems that we have reached the point in our field where advances in understanding interfaces are key: the interface between the radiative interior and the convective envelope, the interface between high and low β environments that exists around the photosphere, and the interface of the corona and the chromosphere through which all coronal field, matter, and energy must travel. These are not easily solved problems, as witnessed by the absence in these proceedings of advances in models of dynamos, of magnetic field behavior within 10,000 km of the photosphere, or of the chromosphere. Have we, in fact, discussed cool-star chromospheres at all in this meeting, apart from the very different ones that exist around (super)giants?

What do we need (compare Dupree and Carpenter in these proceedings)? Clearly multi-wavelength, coordinated observations will help, together with long observing runs, revisiting targets over weeks, months and years (imagine a 5-year movie of a resolved Betelgeuse). New wavelength domains may need to be explored, most notably the infrared. We will benefit from computational and theoretical investments, and from close collaboration between solar and stellar

colleagues. But above all, in our quest to understand what stellar outer atmospheres are all about, we need to have knowledge about the surface magnetic field that tells us about the dynamo, and that determines the mix of the many components that all contribute to the observed signal in our spectrographs. Direct imaging of stars is key to advancing our knowledge of stellar magnetic activity (see *http://hires.gsfc.nasa.gov./∼si/* for a concept of a possible mission).

References

Aschwanden, M., Nightingale, R., & Alexander, D.: 2000, ApJ 541, 1059

Aschwanden, M., Schrijver, C., & Alexander, D.: 2001, ApJ 551, 1036

Ayres, T., Marstad, N., & Linsky, J.: 1981, ApJ 247, 545

Baliunas, S., Donahue, R., Soon, W., & et al.: 1995, ApJ 438, 269

Basu, S., Antia, H., & Tripathy, S.: 1999, ApJ 512, 458

Berger, T., De Pontieu, B., Schrijver, C., & Title, A.: 1999, ApJL 519, 97

Berger, T., Löfdahl, M. , Shine, R., & Title, A.: 1998, ApJ 495, 973

Buzasi, D. : 1997, ApJ 484, 855

Deluca, E., Fan, Y., & Saar, S.: 1997, ApJ 481, 369

DeVore, C.: 1987, SPh 112, 17

Dmitruk, P. & Gomez, D.: 1997, ApJL 484, 83

Dorch, S. & Nordlund, Å.: 2001, A&A 365, 562

Einaudi, G., Velli, M., Politano, H., & Pouquet, A.: 1996, ApJL 457, 113

Fletcher, L. & De Pontieu, B.: 1999, ApJL 520, 135

Galsgaard, K. & Nordlund, Å.: 1996, JGR 101, 13445

Golub, L. & Pasachoff, J.: 1997, *The Solar Corona*, Cambridge University Press, Cambridge, U. K.

González Hernández, I., Patrón, J., Bogart, R., & The SOI Ring Diagram Team: 1999, ApJL 510, L53

Granzer, Th., Schüssler, M., Caligari, P., & Strassmeier, K.: 2000, A&A 355, 1087

Hagenaar, H.: 2001, ApJ 555, 448

Harvey, K.: 1992, in K. Harvey (Ed.), *The Solar Cycle*, Proceedings of the National Solar Observatory / Sacramento Peak 12th summer workshop, Astron. Soc. of the Pacific Conf. Ser. Vol 27, San Francisco, p. 335

Harvey, K.: 1993, *Ph.D. thesis*, Astronomical Institute, Utrecht University

Hathaway, D., Beck, J., Bogart, R., Bachmann, K., Khatri, G., Petitto, J., Han, S., & Raymond, J.: 2000, SPh 193, 299

Heyvaerts, J. & Priest, E.: 1992, ApJ 390, 297

Inverarity, G. & Priest, E.: 1995a, A&A 296, 395

Inverarity, G. & Priest, E.: 1995b, A&A 302, 567

Inverarity, G., Priest, E., & Heyvaerts, J.: 1995, A&A 293, 913

Kitchatinov, L. & Rüdiger, G.: 1995, A&A 299, 446

Klimchuk, J.: 2000, SPh 193, 53

Laming, J., Drake, J., & Widing, K.: 1995, ApJL 443, 416

Lee, J., White, S., Kundu, M., Mikić, Z., & McClymont, A.: 1999, ApJ 510, 413

MacKay, D., Galsgaard, K., Priest, E., & Foley, C.: 2000, SPh 193, 93

Mandrini, C., Démoulin, P., & Klimchuk, J.: 2000, ApJ 530, 999

Mewe, R., Gronenschild, E., & Van den Oord, G.: 1985, A& AS 62, 1985

Mewe, R., Lemen, J., & van den Oord, G.: 1986, A&AS 65, 511

Meyer, J.-P.: 1985, ApJSS 57, 151

Noyes, R., Hartmann, L., Baliunas, S., Duncan, D., & Vaughan, A.: 1984, ApJ 279, 763

Oranje, B., Zwaan, C., & Middelkoop, F.: 1982, A&A 110, 30

Parker, E.: 1983, ApJ 264, 642

Rosner, R., Tucker, W., & Vaiana, G.: 1978, ApJ 220, 643

Saar, S. & Brandenburg, A.: 1999, ApJ 524, 295

Schrijver, C. 2001, ApJ 547, 475 (paper I)

Schrijver, C. & Aschwanden, M.: 2002, ApJ, in press (paper III)

Schrijver, C., Dobson, A., & Radick, R.: 1992, A&A 258, 432

Schrijver, C., Lemen, J., & Mewe, R.: 1989, ApJ 341, 484

Schrijver, C. & Martin, S.: 1990, SPh 129, 95

Schrijver, C. & Title, A.: 2001, ApJ 551, 1099 (paper II)

Schrijver, C., Title, A., Harvey, K., Sheeley, N., Wang, Y., Van den Oord, G., Shine, R., Tarbell, T., & Hurlburt, N.: 1998, Nature 394, 152

Schrijver, C., Title, A., Van Ballegooijen, A., Hagenaar, H., & Shine, R.: 1997, ApJ 487, 424

Schüssler, M., Caligari, P., Ferriz-Mas, A., Solanki, S., & Stix, M.: 1996, A&A 314, 503

Serio, S., Peres, G., Vaiana, G., Golub, L., & Rosner, R.: 1981, ApJ 243, 288

Sheeley, N.: 1992, in K. Harvey (Ed.), *The solar cycle*, A. S. P. Conf. Series, Vol. 27, Astron. Soc. of the Pac., San Francisco, p. 1

Sheeley, N., Bohlin, J., Brueckner, G., Purcell, J., Scherrer, V., & Tousey, R.: 1975, SPh 40, 103

Sheeley, N., Nash, A., & Wang, Y.-M.: 1987, ApJ 319, 481

Strassmeier, K.: 2000, in R. García López, R. Rebolo, and M. Zapatero Osorio (Eds.), *Cool Stars, Stellar Systems and the Sun*, Proc. 11th Cambridge Workshop, Astron. Soc. Pac. Conference Series, Volume 223, p. 271

Tobias, S. M., Brummell, N. H., Clune, Th. L., & Toomre, J.: 2001, ApJ 549, 1183

Van den Oord, G., Schrijver, C., Camphens, M., Mewe, R., & Kaastra, J.: 1997, A&A 326, 1090

Vogt, S., Hatzes, A., & Misch, A.: 1999, ApJSS 121, 547

Watko, J. & Klimchuk, J.: 2000, SPh 193, 77

Zwaan, C.: 1981, in R. Bonnet and A. Dupree (Eds.), *Solar Phenomena in Stars and Stellar Systems*, NATO-ASI, Bonas, D. Reidel, Dordrecht, The Netherlands, p. 463